

Supplementary Materials for

Massive Phytoplankton Blooms Under Arctic Sea Ice

Kevin R. Arrigo,^{1*} Donald K. Perovich,^{2,3} Robert S. Pickart,⁴ Zachary W. Brown,¹ Gert L. van Dijken,¹ Kate E. Lowry,¹ Matthew M. Mills,¹ Molly A. Palmer,¹ William M. Balch,⁵ Frank Bahr,⁴ Nicholas R. Bates,⁶ Claudia Benitez-Nelson,⁷ Bruce Bowler,⁵ Emily Brownlee,⁸ Jens K. Ehn,⁹ Karen E. Frey,¹⁰ Rebecca Garley,⁶ Samuel R. Laney,⁸ Laura Lubelczyk,⁵ Jeremy Mathis,¹¹ Atsushi Matsuoka,¹² B. Greg Mitchell,⁹ G. W. K. Moore,¹³ Eva Ortega-Retuerta,¹⁴ Sharmila Pal,⁷ Chris M. Polashenski,² Rick A. Reynolds,⁹ Brian Schieber,⁹ Heidi M. Sosik,⁸ Michael Stephens,¹⁵ James H. Swift⁹

¹Department of Environmental Earth System Science, Stanford University, Stanford, CA 94305, USA.

²Engineer Research and Development Center, Cold Regions Research and Engineering Laboratory, Hanover, NH 03755, USA. ³Thayer School of Engineering, Dartmouth College, Hanover, NH 03755, USA. ⁴Department of Physical Oceanography, Woods Hole Oceanographic Institution, Woods Hole, MA 02543, USA. ⁵Bigelow Laboratory for Ocean Sciences, West Boothbay Harbor, ME 04575, USA.

⁶Bermuda Institute of Ocean Sciences, Ferry Reach GE01, Bermuda. ⁷Marine Science Program and Department of Earth and Ocean Sciences, University of South Carolina, Columbia, SC 29208, USA.

⁸Biology Department, Woods Hole Oceanographic Institution, Woods Hole, MA 02543, USA. ⁹Scripps Institution of Oceanography, University of California San Diego, La Jolla, CA 92093, USA. ¹⁰Graduate School of Geography, Clark University, Worcester, MA 01610, USA. ¹¹School of Fisheries and Ocean Sciences, University of Alaska Fairbanks, Fairbanks, AK 99775, USA. ¹²Universite Pierre et Marie Curie, Laboratoire d'Océanographie de Villefranche, Villefranche-sur-Mer 06238, France. ¹³Department of Physics, University of Toronto, Toronto, Ontario M5S 1A7, Canada. ¹⁴Laboratoire d'Océanographie Microbienne, Observatoire Océanologique, Centre Nationale de la Recherche Scientifique et Université Paris Pierre et Marie Curie, Banyuls/Mer 66650, France. ¹⁵Colby College, Waterville, ME 04901, USA.

*To whom correspondence should be addressed. E-mail: arrigo@stanford.edu

Published 7 June 2012 on *Science Express*

DOI: 10.1126/science.1215065

This PDF file includes:

Materials and Methods
Figs. S1 and S2
References

Materials and Methods

Samples for fluorometric analysis of Chl *a* were filtered onto 25 mm Whatman GF/F filters (nominal pore size 0.7 μm) placed in 5 mL of 90% acetone, and extracted in the dark at 3°C for 24 hrs. Chl *a* was measured fluorometrically (8) using a Turner Fluorometer 10-AU (Turner Designs, Inc.).

Particulate organic carbon samples were collected by filtering sub-samples onto pre-combusted (450°C for 4 hrs) 25 mm Whatman GF/F filters. The filters were immediately dried at 60°C and stored dry until analysis. Prior to analysis, the samples were fumed with concentrated HCl, dried at 60°C, and packed into tin capsules (Costech Analytical Technologies, Inc.) for elemental analysis on a Carlo-Erba NA-1500 elemental analyzer. Peach leaves and glutamic acid were used as a calibration standard.

The maximum efficiency of photosystem II (Fv:Fm) was determined by fast repetition rate fluorometry (FRRf) (9) on samples collected with Niskin bottles. Samples were dark acclimated for ~30 min at in situ temperatures before measurement with the FRRf. Blanks for individual samples analyzed by FRRf were prepared by gentle filtration through a 0.2 μm polycarbonate syringe filter before measurement using identical protocols. All Fv:Fm values were corrected for blank effects (10).

Photosynthesis versus irradiance relationships (P^*_m , α^* , E_k) were determined using a modified ^{14}C -bicarbonate incorporation technique (11-12). Carbon uptake, normalized by Chl *a* concentration, was calculated from radioisotope incorporation, and the data were fit by least squares nonlinear regression (13). P-E parameters were used with under-ice light profiles to estimate rates of depth-integrated daily gross primary production. Specific growth rate (μ , d^{-1}) in surface waters was calculated by multiplying the photosynthetic rate (P^*) by the POC:Chl *a* ratio.

Water samples collected from Niskin bottles were analyzed for nitrate (NO_3) and nitrite (NO_2) concentrations with a Seal Analytical continuous-flow AutoAnalyzer 3 (AA3) using a modification of the Armstrong *et al.* (14) procedure. For the NO_3 analysis, seawater samples were passed through a cadmium reduction column where NO_3 was quantitatively reduced to NO_2 . Sulfanilamide was then introduced to the sample stream followed by N-(1-naphthyl) ethylenediamine dihydrochloride which couples to form a red azo dye. The stream was then passed through a flow cell and the absorbance measured at 520 nm. The same technique was employed for NO_2 analysis,

except the cadmium column was bypassed. Absorbance vs. concentration standard curves were used to determine the molar concentration of the combined $[\text{NO}_3+\text{NO}_2]$ and NO_2 alone.

Seawater samples for DIC were drawn from the Niskin samplers into pre-cleaned ~300 mL borosilicate bottles, poisoned with HgCl_2 to halt biological activity, sealed, and returned to the Bermuda Institute of Ocean Sciences (BIOS) for analysis. DIC samples were analyzed using a highly precise ($\sim 0.025\%$; $< 0.5 \text{ mmol kg}^{-1}$) gas extraction/coulometric detection system (15). Analyses of Certified Reference Materials (provided by A. G. Dickson, Scripps Institution of Oceanography) ensured that the accuracy of the DIC and TA measurements was 0.05% ($\sim 0.5 \text{ mmol kg}^{-1}$) and 0.1% ($\sim 2 \text{ mmol kg}^{-1}$), respectively.

Phytoplankton assemblage composition was examined using imaging-in-flow cytometry, where high-speed photomicrographs of individual cells and chains were identified to the genus level or better using automated classification (16) followed by manual verification.

Fig. S1. MODIS-Aqua satellite image of the northern Chukchi Sea showing the distribution of sea ice on 8 July 2011 and the location of stations sampled during the ICESCAPE 2011 cruise. Black indicates open water. Lines show the position of the ice edge on the indicated dates (AMSR-E). Stations 46-57 are part of Transect 1 and stations 57-71 are Transect 2.

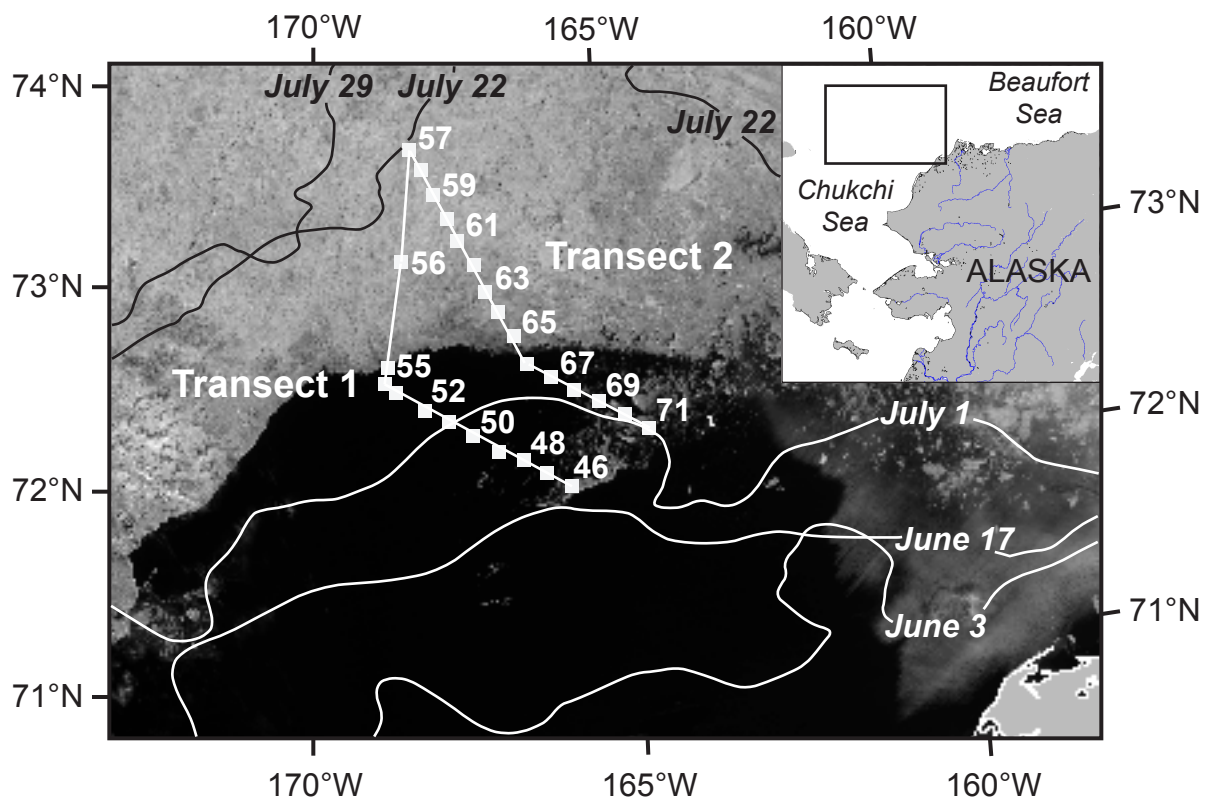


Fig. S1

References and Notes

1. K. R. Arrigo, G. L. van Dijken, Secular trends in Arctic Ocean net primary production. *J. Geophys. Res.* **116**, C09011 (2011). [doi:10.1029/2011JC007151](https://doi.org/10.1029/2011JC007151)
2. Materials and methods are available as supplementary materials on *Science Online*.
3. J. Zhang *et al.*, Modeling the impact of declining sea ice on the Arctic marine planktonic ecosystem. *J. Geophys. Res.* **115**, C10015 (2010). [doi:10.1029/2009JC005387](https://doi.org/10.1029/2009JC005387)
4. V. H. Strass, E.-M. Nöthig, Seasonal shifts in ice edge phytoplankton blooms in the Barents Sea related to the water column stability. *Polar Biol.* **16**, 409 (1996). [doi:10.1007/BF02390423](https://doi.org/10.1007/BF02390423)
5. C. J. Mundy *et al.*, Contribution of under-ice primary production to an ice-edge upwelling phytoplankton bloom in the Canadian Beaufort Sea. *Geophys. Res. Lett.* **36**, L17601 (2009). [doi:10.1029/2009GL038837](https://doi.org/10.1029/2009GL038837)
6. M. Fortier, L. Fortier, C. Michel, L. Legendre, Climatic and biological forcing of the vertical flux of biogenic particles under seasonal Arctic sea ice. *Mar. Ecol. Prog. Ser.* **225**, 1 (2002). [doi:10.3354/meps225001](https://doi.org/10.3354/meps225001)
7. O. Holm-Hansen, C. J. Lorenzen, R. W. Holmes, J. D. H. Strickland, Fluorometric determination of chlorophyll. *ICES J. Mar. Sci.* **30**, 3 (1965). [doi:10.1093/icesjms/30.1.3](https://doi.org/10.1093/icesjms/30.1.3)
8. Z. S. Kolber, O. Prasil, P. G. Falkowski, Measurements of variable chlorophyll fluorescence using fast repetition rate techniques: Defining methodology and experimental protocols. *Biochimica Biophysica Acta Bioenergetics* **1367**, 88 (1998). [doi:10.1016/S0005-2728\(98\)00135-2](https://doi.org/10.1016/S0005-2728(98)00135-2)
9. J. J. Cullen, R. F. Davis, *Limnol. Oceanogr. Bull.* **12**, 29 (2003).
10. M. R. Lewis, J. C. Smith, A small volume, short-incubation-time method for measurement of photosynthesis as a function of incident irradiance. *Mar. Ecol. Prog. Ser.* **13**, 99 (1983). [doi:10.3354/meps013099](https://doi.org/10.3354/meps013099)
11. K. R. Arrigo *et al.*, Photophysiology in two major Southern Ocean phytoplankton taxa: Photosynthesis and growth of *Phaeocystis antarctica* and *Fragilariopsis cylindrus* under different irradiance levels. *Integr. Comp. Biol.* **50**, 950 (2010). [doi:10.1093/icb/icq021](https://doi.org/10.1093/icb/icq021)
[Medline](#)
12. T. Platt, C. L. Gallegos, W. G. Harrison, *J. Mar. Res.* **38**, 687 (1980).
13. F. A. J. Armstrong, C. R. Stearns, J. D. H. Strickland, *Deep-Sea Res.* **14**, 381 (1967).
14. N. R. Bates, M. H. P. Best, D. A. Hansell, Spatio-temporal distribution of dissolved inorganic carbon and net community production in the Chukchi and Beaufort Seas. *Deep Sea Res. Part II Top. Stud. Oceanogr.* **52**, 3303 (2005). [doi:10.1016/j.dsr2.2005.10.005](https://doi.org/10.1016/j.dsr2.2005.10.005)
15. H. M. Sosik, R. J. Olson, Automated taxonomic classification of phytoplankton sampled with imaging in-flow cytometry. *Limnol. Oceanogr. Methods* **5**, 204 (2007). [doi:10.4319/lom.2007.5.204](https://doi.org/10.4319/lom.2007.5.204)